

# Multiple-Retrapping Process in High- $T_c$ Intrinsic Josephson Junctions

Myung-Ho Bae<sup>1,\*</sup>, M. Sahu<sup>1</sup>, Hu-Jong Lee<sup>2</sup>, and A. Bezryadin<sup>1,†</sup>

<sup>1</sup>*Department of Physics, University of Illinois at Urbana-Champaign, Urbana, Illinois 61801-3080, USA and*

<sup>2</sup>*Department of Physics, Pohang University of Science and Technology, Pohang 790-784, Republic of Korea*

(Dated: February 2, 2022)

We report measurements of switching-current distribution (SWCD) from a phase-diffusion branch to a quasiparticle-tunneling branch as a function of temperature in a cuprate-based intrinsic Josephson junction. Contrary to the thermal-activation model, the width of the SWCD increases with decreasing temperature, down to 1.5 K. Based on the multiple-retrapping model, we quantitatively demonstrate that the quality factor of the junction in the phase-diffusion regime determines the observed temperature dependence of the SWCD.

PACS numbers: 74.72.Hs, 74.50.+r, 74.40.+k, 74.45.+c

The escape of a system trapped in a metastable state governs the reaction rate in various dynamical systems, where the escape is made by a noise-assisted hopping [1]. In the case of a Josephson junction (JJ), a thermal noise induces an escape of a phase particle representing the system from a local minimum of the potential well. In an underdamped JJ with hysteresis in the voltage-current ( $V$ - $I$ ) characteristics a single escaping event induces a switching from a zero-voltage phase-trapped state to a finite-voltage phase-rolling state [2]. In an overdamped JJ without hysteresis, however, the energy of an escaped phase particle is dissipated during its motion so that the particle is retrapped in another local minimum of the potential. The phase particle repeats this thermally activated escape and retrapping process, *i.e.*, the multiple-retrapping process. It results in a phase-diffusion branch (PDB); a resistive branch with a small but finite voltage for a bias current below a switching current,  $I_{SW}$  [3].

A hysteretic JJ can also evolve into this multiple-retrapping state with increasing temperature ( $T$ ) when the energy fed by a bias current, near a mean switching current that is suppressed by an increment in  $T$ , gets comparable to the dissipated energy. Recently, this phase-retrapping phenomenon in the hysteretic JJ has been intensively studied in association with the  $T$  dependence of a switching current distribution (SWCD) [4, 5]. The main finding of these studies is that the retrapping process in the hysteretic JJ modifies the switching dynamics, in such a way as to *reduce the width of SWCD with increasing  $T$* . This SWCD behavior, contrasting to the usual thermal activation model, has also been suggested to be caused by the enhanced dissipation due to a high-frequency impedance, which originates from the contribution of the impedance of the measurement lines [6, 7], incorporating into temperature effect [8]. At sufficiently high  $T$ , the hysteretic JJ begins to show a PDB. This PDB in a hysteretic JJ can be found whenever the thermal energy,  $k_B T$ , is comparable to the Josephson energy,  $E_J$  ( $=\hbar I_c/2e$ ;  $I_c$  is the noise-free critical current and  $k_B$  is the Boltzmann constant). Thus, an ultra-small hysteretic JJ exhibits the PDB even at a-few-mK

region [9]. As the dissipation is represented by the quality factor  $Q$  of the JJ, however, it has not been clearly resolved yet how  $Q$ , depending both on the temperature and the impedance, affects switching between a PDB and a quasiparticle-tunneling branch (QTB).

In this letter, we study switching from the PDB to the QTB in intrinsic Josephson junctions (IJJs) of  $\text{Bi}_2\text{Sr}_2\text{CaCu}_2\text{O}_{8+x}$  (Bi-2212) at various temperatures. The effective junction impedance  $Z_J$  including the influence of an external circuit in a PDB, was estimated by fitting  $V$ - $I$  curves to the phase-diffusion model. The values of  $Z_J$  turn out to be an order of the measurement-line impedance  $Z_L$ , which indicates that the phase dynamics of our IJJs is governed by the environmental dissipation. Our measurements of the  $T$  dependence of the switching rate  $\Gamma_S$  and the corresponding SWCD in a single IJJ are in good agreement with those estimated by the multiple-retrapping model. This study quantitatively clarifies how the impedance- and temperature-related dissipations, and the corresponding  $Q$  determine the switching dynamics in a hysteretic IJJ with phase-diffusion characteristics.

A stack with the lateral size of  $2.5 \times 2.9 \mu\text{m}^2$  in Bi-2212 single crystal was defined by using focused-ion-beam (FIB) process [10]. High-intensity FIB irradiation is known to degrade the peripheral region by the scattered secondary ion beam [11]. In the milling process, we used a relatively high ion-beam current of 3 nA, corresponding to  $\sim 200 \text{ pA}/\mu\text{m}^2$ . This high ion-beam current much reduced the interlayer tunneling critical current density down to  $\sim 8 \text{ A}/\text{cm}^2$  in  $N=12$  junctions out of total  $\sim 100$  junctions in a stack, which were estimated from the number of QTBs in  $V$ - $I$  curves of the stack. Four-terminal transport measurements were carried out in a pumped  $\text{He}^4$  dewar with the base temperature of 1.45 K. Room-temperature  $\pi$ -filters were employed and measurement lines were embedded in silver paste at cryogenic temperatures to suppress high-frequency noises propagating along the leads. The measurements were made by using battery-operated low-noise amplifiers (PAR-113). The ramping speed of the bias current and the threshold volt-

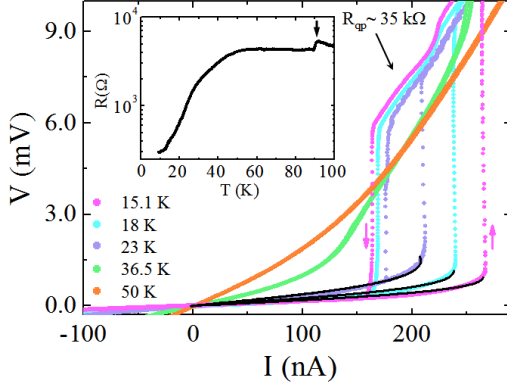


FIG. 1: (color online)  $V$ - $I$  characteristics at various temperatures of the Bi-2212 IJJs stack. The upward and downward arrows indicate the switching and the return currents, respectively, at  $T=15.1$  K. Black solid curves are the best fits to the phase diffusion model at three different temperatures of 15.1 K, 18 K, and 23 K, with the effective junction impedance  $Z_J=125$ , 125, and 128  $\Omega$  as the best-fit parameters, respectively. Inset: the  $R$ -vs- $T$  curve, where  $T_c$  is indicated by an arrow.

age (obtained from the maximum voltage of the PDB) in measuring  $I_{SW}$  were  $\dot{I}=30$   $\mu\text{A}/\text{sec}$  and  $V_{th}=110$   $\mu\text{V}$  [12], respectively. Measurements were made on the first jump, which connected the PDB to the first QTB of the weakest junction in the stack. For each distribution, 10000 switching events were recorded with the current resolution of 90 pA.

The inset of Fig. 1 shows the tunneling  $R$  vs  $T$  curves with the superconducting transition at  $T_c=90$  K, which is indicated by an arrow. The  $c$ -axis tunneling nature in the Bi-2212 stacked junctions is evident by the increasing resistance with decreasing  $T$  above  $T_c$ . At  $T < T_c$ , the junction resistance does not vanish completely, even down to  $T=10$  K, which is attributed to the phase diffusion in the junctions. Fig. 1 shows the  $V$ - $I$  curves at various  $T$  below  $T_c$ . The nonlinear curve at  $T=50$  K begins to show a hysteresis below  $T \sim 30$  K. For a bias below a  $I_{SW}$  in each curve, a pronounced non-zero resistive branch appears below  $T=23$  K. Here, the finite resistance is caused by the phase diffusion in the condition of  $k_B T \sim 2E_J$  [3]. The phase-diffusion model [13, 14] predicts the current-voltage relation of  $I(V) = \frac{4eI_{SW}k_B T}{\hbar} \frac{Z_J v}{v^2 + [2eZ_J k_B T/\hbar]^2}$  with a frequency-dependent effective junction impedance  $Z_J$ . Here, the phase diffusion is assumed to take place in all twelve junctions with FIB-suppressed critical currents, so that the voltage bias per junction becomes  $v = V/N$ . We use this relation to fit the PDB as shown by black curves in Fig. 1 with  $Z_J$  as the best-fit parameter.  $Z_J$  turns out to be 125, 125, and 128  $\Omega$  for  $T=15.1$ , 18, and 23 K, respectively. These values of  $Z_J$  are comparable to the measurement line impedance  $Z_L$  (50~100  $\Omega$ ), even with a much higher quasiparticle tunneling resistance of  $R_{qp} \sim 35$

k $\Omega$  as seen in Figure 1. This implies that the dissipation in the PDB is dominated by the high-frequency (of an order of the Josephson plasma frequency,  $\omega_p$ ) dissipation through the measurement lines [6, 7]. Since the energy of the escaped phase particle is dissipated through the environment in the phase-diffusive regime, the switching also becomes sensitive to this dissipation process.

Now, we turn to the switching event from the PDB to the QTB. Fig. 2(a) shows the SWCD (scattered symbols) at various temperatures. The standard deviation ( $\sigma$ ) and the mean switching currents ( $\langle I_{SW} \rangle$ ) are shown as a function of  $T$  in the inset of Fig. 2(a). The  $T$  dependence of  $\sigma$  contradicts to that of a conventional underdamped JJ, where  $\sigma$  increases with  $T$  in a thermal-activation regime [2]. Fig. 2(b) shows  $\Gamma_S$  (scattered points) vs  $I$  calculated from the SWCD of Fig. 2(a) following the Fulton and Dunkleberger analysis [2]. With lowering  $T$ ,  $\Gamma_S(I)$  shows a pronounced change from an almost linear to a down-turn nonlinear bias-current dependence in a semi-logarithmic plot. To explain this behavior, we adopted the multiple-retrapping model [5, 8]. In the phase-diffusive regime, the successive retrapping processes suppress the switching rate,  $\Gamma_S$ . The switching to the high-voltage branch (i.e. the QTB) occurs only when the phase particle is not retrapped after escaping from a local energy minimum. A phase particle escaped from a potential minimum has a probability,  $P_{RT}$ , to be retrapped in the next potential minimum. The switching rate  $\Gamma_S$ , including  $P_{RT}$ , is expressed by [8]

$$\Gamma_S = \Gamma_{TA}(1 - P_{RT}) \frac{\ln(1 - P_{RT})^{-1}}{P_{RT}}. \quad (1)$$

Here,  $\Gamma_{TA} [= \frac{\omega_p}{2\pi} \exp(-\frac{\Delta U}{k_B T})]$  is the thermally activated escape rate,  $\omega_p = \omega_{p0}(1 - \gamma^2)^{1/4}$ ,  $\omega_{p0} = (2eI_c/\hbar C)^{1/2}$ ,  $\Delta U(\phi) [= 2E_J((1 - \gamma^2)^{1/2} - \gamma \arccos \gamma)]$  is the escape energy barrier, and  $\gamma [= I/I_c]$  is a normalized bias current. The retrapping probability can be obtained by an integration (see Ref. [15]) of the retrapping rate  $\Gamma_{RT} = \frac{1}{Z_J C} (\Delta U_{RT}/\pi k_B T)^{1/2} \exp(-\Delta U_{RT}/k_B T)$ , where  $\Delta U_{RT}(I) = Z_J^2 C (I - I_{r0})^2$  and  $I_{r0}$  is the noise-free return current from a QTB to a PDB [16]. Fig. 3(a) shows the experimental switching distribution (red dots) at  $T=1.5$  K with the corresponding fit (green curve) obtained by using Eq. (1) with the best-fit parameters of  $Z_J=61.9$   $\Omega$ ,  $I_c=1.26$   $\mu\text{A}$ , and  $I_{r0}=63$  nA. The junction capacitance, 330 fF, was estimated from the typical value of 45 fF/ $\mu\text{m}^2$  for Bi-2212 IJJs [17]. The corresponding switching rate (red dots) and the fit (green curve) are shown in Fig. 3(b), with the same parameters. An excellent agreement is obtained in both fittings.

These results are analyzed in terms of  $Z_J$ - and  $T$ -dependence of  $P_{RT}$ . The inset of Fig. 3(a) shows the calculated  $P_{RT}$ -vs- $I$  curves for various  $Z_J$  at  $T=1.5$  K, with the values of  $I_c$  and  $I_{r0}$  obtained from the best fits of Figure 3. The retrapping-probability curve shifts to

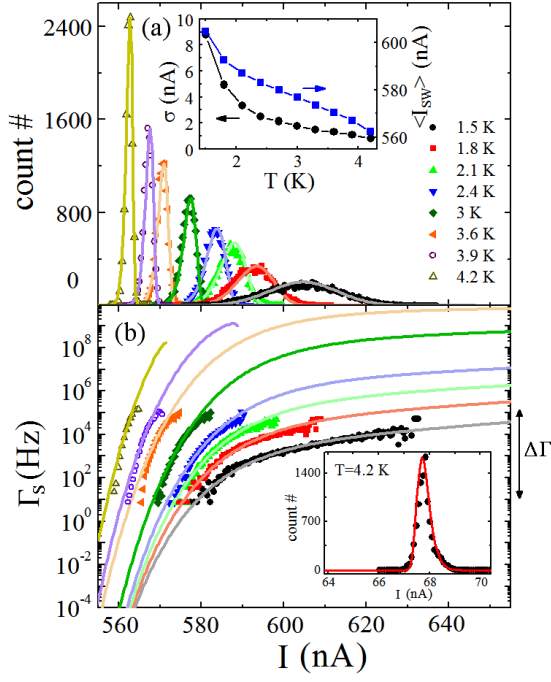


FIG. 2: (color online) (a) The switching current distribution and (b) the corresponding  $\Gamma_S$  at various  $T$  from 1.5 K to 4.2 K. The solid lines are calculated based on the multiple-retrapping model. Inset: Temperature dependence of the standard deviation ( $\sigma$ ) and the mean switching current ( $\langle I_{SW} \rangle$ ).  $\Delta\Gamma$  is the range of the observable switching rate for a given  $\dot{I}_b$ . Inset: the re trapping current distribution (solid circles) and the calculated behavior (solid line) at  $T=4.2$  K.

higher currents as  $Z_J$  decreases, due to the presence of a  $Z_J$  dependence of  $\Delta U_{RT}$  in the exponential factor of  $\Gamma_{RT}$ . The current positions of almost vanishing  $P_{RT}$ , indicated by downward arrows, approximately correspond to the maximum current allowing the retrapping. We denote this current as  $I_{PD}$ . Physically this is the same current as the one denoted  $I_m$  in Ref. [6]. The system can hardly be retrapped at a current higher than  $I_{PD}$ , because in this case the energy fed to the system by the bias current gets larger than the dissipated energy. By equating the energy fed and the energy dissipated, similar to McCumber and Stewart analysis [4], one obtains the relation

$$I_{PD} = 4I_c / \pi Q_{PD}, \quad (2)$$

where  $Q_{PD}$  is the phase-diffusion quality factor at  $\omega \sim \omega_p$  [6]. In fact, the noise-free retrapping current can be written in a form similar to Eq. (2), namely as  $I_{r0} = 4I_c / \pi Q(\omega=0)$  [3]. The thick black curves in Figs. 3(a) and 3(b) show SWCD and the corresponding  $\Gamma_{TA}(I)$ , respectively. Other solid curves in Fig. 3(b) are  $\Gamma_S(I)$  in Eq. (1) for varying  $Z_J$  under the multiple retrapping processes.  $\Gamma_S(I)$  with each  $Z_J$  in Fig. 3(b) starts to drop quickly from  $\Gamma_{TA}(I)$  at  $I=I_{PD}$ , which are denoted by

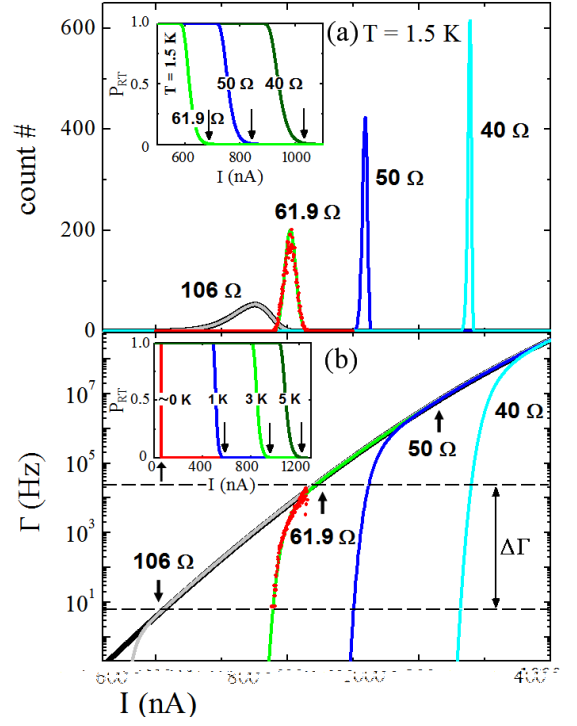


FIG. 3: (color online) (a) The solid lines represent the calculated switching current distributions for various  $Z_J$  values of 106, 61.9, 50, and 40  $\Omega$ , corresponding to  $Q_{PD}=3.88, 2.37, 1.90$  and  $1.55$ , respectively. Red dots show the SWCD at  $T=1.5$  K. Inset: Theoretical retrapping probabilities versus bias current, for various  $Z_J$  values at  $T=1.5$  K. The downward arrows indicate the  $I_{PD}$  values. (b) Estimated switching rate versus the bias current. Red dots correspond to the experimental switching rate for  $T=1.5$  K. Estimated  $\Gamma_S$  for various  $Z_J$  values in Eq. (1) are shown as solid lines. Inset: Estimated retrapping probabilities versus bias current with  $Z_J=61.9$   $\Omega$  at various  $T$ . Thick black curves in (a) and (b) show the thermally activated switching current distribution and the corresponding escape rate, respectively, without retrapping.

arrows in the figure. We define  $I_{PD}$  as the current value corresponding to  $P_{RT}=0.01$ , where  $\Gamma_S(I_{PD})$  is nearly the same as the  $\Gamma_{TA}(I_{PD})$  as shown in Fig. 3(b) [8]. The impedance of 106  $\Omega$  gives the same SWCD as thermally activated SWCD without retrapping because  $\Gamma_S(I)$  in  $\Delta\Gamma$  well overlaps with  $\Gamma_{TA}(I)$  although the impedance is of an order of  $Z_L$ . When  $\Gamma_S(I_{PD})$  crosses over the bottom line of  $\Delta\Gamma$  while  $Z_J$  keeps decreasing, the high-frequency dissipation affects the SCDW: the observable window of  $\Delta\Gamma$  (between the two dashed lines) for a fixed  $\dot{I}_b$  shifts to the steeper section with decreasing  $Z_J$ , resulting in the decreasing width of the SWCD in Figure 3(a) at a constant  $T$ . This shift itself is caused by a reduction of  $Q_{PD}$  with decreasing  $Z_J$  at a constant  $T$ .

Since  $I_{PD}$  is also affected by a change in  $T$  as followings, the shape of  $\Gamma_S(I)$  dose not simply follow the variation of  $Z_J$  as  $T$  changes. The inset of Fig. 3(b)

TABLE I: Fitting parameters for the switching events for selected temperatures

$T(K)$	$I_c(\mu A)$	$I_{r0}(nA)$	$Z_J(\Omega)$	$I_{PD}(nA)$	$Q_{PD}$
1.5	1.263	63.00	61.9	678	2.37
2.4	1.209	65.10	77.6	683	2.25
3.0	1.006	63.44	86.0	685	1.87
3.6	0.735	65.22	94.7	682	1.37
4.2	0.572	63.79	101.5	572	1.27

illustrates  $P_{RT}$  vs  $I$  at various temperatures. Here,  $Z_J$  is fixed at 61.9  $\Omega$  and other parameters, except for  $T$ , are set to be the same as for the inset of Fig. 3(a). The current position of the zero-temperature curve, indicated by an upward arrow in the inset of Fig. 3(b), corresponds to the fluctuation-free return current  $I_{r0}$ . The value of  $I_{PD}$  shown by arrows increases with increasing  $T$ . Thus, in effect, the retrapping probability curve shifts to higher currents as  $T$  is raised, due to the presence of a Boltzmann-type exponential factor in the expression of  $\Gamma_{RT}$ . Fig. 2 illustrates the calculated SWCD and  $\Gamma_S(I)$  as solid curves at various temperatures with the best-fit parameters listed in Table I, which agree well with the observation. Here, since the dissipation effect by temperature is already determined by a bath temperature, the main fit-parameter becomes  $Z_J$  in Figure 3(a). As shown in Fig. 2(b), with increasing  $T$ , the calculated  $\Gamma_S(I)$  in the window of  $\Delta\Gamma$  shows steeper regions. It causes the reduction of the width of SWCD with decreasing temperature. The ratio of  $I_c$  and  $I_{PD}$  becomes smaller with increasing  $T$  as in Table I.  $I_{PD}$  even equals to  $I_c$  at  $T=4.2$  K. This behavior leads to the conclusion that  $Q_{PD}$  decreases with increasing  $T$  following Eq. (2) despite the increase of  $Z_J$  with  $T$  [18]. The slope of the calculated  $\Gamma_S(I)$  in the window of  $\Delta\Gamma$  at sufficiently high temperatures is insensitive to  $T$  variations, which leads to the saturation of  $\sigma$  with increasing  $T$  as the inset of Figure 2(a).

Now we consider the retrapping dynamics related to the transition from a QTB to a PDB in an underdamped JJ. It can be shown that only the zero-frequency dissipation plays an significant role in the retrapping dynamics [6]. The inset of Fig. 2(b) shows the stochastic nature of the retrapping current as shown by solid circles at  $T=4.2$  K. The calculated retrapping distribution (solid line) by the retrapping rate,  $\Gamma_{RT}$ , is consistent with the experimental result. The best-fit parameters are  $I_{r0}=63.8$  nA and  $Z_J=10$  k $\Omega$  ( $\sim R_{qp}$ ), where the estimated noise-free  $I_{r0}$  matches with the value used in  $\Gamma_S$  fitting in Table I. The junction impedance  $Z_J$  estimated from the return currents is significantly larger than  $Z_J$  ( $\omega \sim \omega_p$ ) for the observed switching events. It indicates that the retrapping phenomena from QTB to PDB are mainly determined by a zero-frequency damping with  $Q(0)=11.4$  with  $I_c=572$  nA and  $I_{r0}=63.8$  nA at  $T=4.2$  K as shown in Table I.

In summary, we clearly show that the multiple retrapping processes in underdamped IJJs, with much suppressed critical current and high tunneling resistance, govern the switching from the PDB to the QTB. The predicted SWCD and  $\Gamma_S$  in the multiple-retrapping model are in good agreement with the observed broadening of the distribution of switching currents with decreasing temperature. We also demonstrate that the change of the shapes of the observed SWCD and the  $\Gamma_S$  in various temperatures can be understood by impedance and temperature dependence of  $Q_{PD}$ , taking the retrapping probability into account. As the macroscopic quantum tunneling has been observed recently in IJJs of Bi-2212 single crystals [19], this study provides in a quantitative manner the role of the dissipation in quantum devices based on cuprate-based JJs.

This work was supported by DOE Grants No. DEFG02-07ER46453. We acknowledge the access to the fabrication facilities at the Frederick Seitz Materials Research Laboratory. This work was also partially supported by POSTECH Core Research Program, Acceleration Research Grant No. R17-2008-007-01001-0, and the Korea Research Foundation Grants No. KRF-2006-352-C00020.

\*mhbae@uiuc.edu, †bezryadi@uiuc.edu

- 
- [1] P. Hänggi, P. Talkner, and M. Borkovec, *Rev. Mod. Phys.* **62**, 251 (1990).
  - [2] T. A. Fulton and L. N. Dunkleberger, *Phys. Rev. B* **9**, 4760 (1974).
  - [3] M. Tinkham, *Introduction to Superconductor*, 2nd ed. (McGraw-Hill, New York, 1996).
  - [4] J. M. Kivioja *et. al.*, *Phys. Rev. Lett.* **94**, 247002 (2005).
  - [5] V. M. Krasnov *et. al.*, *Phys. Rev. Lett.* **95**, 157002 (2005); V. M. Krasnov *et. al.*, *Phys. Rev. B* **76**, 224517 (2007).
  - [6] J. M. Martinis and R. L. Kautz, *Phys. Rev. Lett.* **63**, 1507 (1989); R. L. Kautz and J. M. Martinis, *Phys. Rev. B* **42**, 9903 (1990).
  - [7] A. T. Johnson, C. J. Lobb, and M. Tinkham, *Phys. Rev. Lett.* **65**, 1263 (1990).
  - [8] J. Männik *et. al.*, *Phys. Rev. B* **71**, R220509 (2005).
  - [9] D. Vion *et. al.*, *Phys. Rev. Lett.* **77**, 3435 (1996).
  - [10] S. J. Kim *et. al.*, *Appl. Phys. Lett.* **74**, 1156 (1999).
  - [11] M.-H. Bae *et. al.*, *Phys. Rev. B* **77**, 144501 (2008).
  - [12] In our measurement setup, the voltage spacing between the maximum voltage value of the PDB and the next jumping voltage is  $\sim 150$   $\mu$ V so that the value of our  $V_{th}$  of 110  $\mu$ V is reasonable to obtain  $I_{SW}$  values.
  - [13] G.-L. Ingold, H. Grabert, and U. Eberhardt, *Phys. Rev. B* **50**, 395 (1994).
  - [14] A. Franz *et al.*, *Phys. Rev. B* **69**, 014506 (2004).
  - [15] A. Garg, *Phys. Rev. B* **51**, 15592 (1995). The retrapping current distribution with increasing bias current is given by the Kurkijärvi-Fulton-Dunkleberger formula,  $P(I) = \frac{\Gamma_{RT}}{dI/dt} \exp[-\int_I^{I_c} \frac{\Gamma_{RT}(I')}{dI'/dt} dI']$  and the retrapping probability at  $I$  is obtained by  $P_{RT}(I) =$

$$\int_I^{I_c} P(I') dI' / \int_0^{I_c} P(I') dI'.$$

- [16] E. Ben-Jacob *et al.*, Phys. Rev. A **26**, 2805 (1982).
- [17] A. Irie, Y. Hirai, and G. Oya, Appl. Phys. Lett **72**, 2159 (1998).
- [18] The noise-free critical current,  $I_c$ , is strongly suppressed with  $T$ , resulting in a reduction of  $\omega_p$ . Thus, the frequency related to a phase diffusion dynamics gets smaller, leading to a larger value of  $Z_J$  with  $T$  as shown in Table I [6].
- [19] K. Inomata *et. al.*, Phys. Rev. Lett. **95**, 107005 (2005); X. Y. Jin *et. al.*, Phys. Rev. Lett. **96**, 177003 (2006); S.-X. Li *et. al.*, Phys. Rev. Lett. **99**, 037002 (2007).